Effect of CaF_2 addition on the densification behavior and mechanical properties of resistant anorthite and its bioactivity

S. Zaiou[a,b], O. Beldjebli[c], D. Belfennache[d,*], M.Tayeb[e], F. Zenikheri[f], A. Harabi[c]
[a]*Emergent Materials Research Unit, Setif 1 University, 19000 Setif, Algeria*
[b]*Faculty of Natural Sciences and Life, Setif 1 University, 19000 Setif, Algeria*
[c]*Ceramics Laboratory, Physics Department, Faculty of Exact Sciences, Mentouri Brothers-Constantine 1 University, 25000 Constantine, Algeria*
[d]*Research Center in Industrial Technologies CRTI, P.O. Box 64, Cheraga, 16014 Algiers, Algeria*
[e]*Young Researchers and Elites Club, Science and Research Branch, Islamic Azad University, Tehran, Iran*
[f]*Higher Normal School of Technological Education, Skikda, Algeria*

In the current study, anorthite ceramic (CaO, Al_2O_3, $2SiO_2$) was synthesized by a simple solid-state reaction method, using local Algerian raw materials. The effect of sintering temperature at 800, 850, 900, 950, 1000, and 1100 °C for 1h under atmosphere, and 0.5, 1.5, and 3 wt % calcium fluoride (CaF_2) addition on the densification and mechanical properties of anorthite were studied. The correlation between these properties and the bioactivity of samples was investigated. The results showed that samples with 1.5 wt.% CaF_2 sintered at 900 °C has the highest bulk density (2.7 $g.cm^{-3}$), lowest apparent porosity (3%), outstanding micro-hardness (8.7 GPa), and high flexural strength (222 MPa) of anorthite. The in vitro bioactivity test was assessed by determining the changes in surface composition and morphology after immersion in a simulated body fluid (SBF) for 8 h to 21 days. The results of the bioactivity test determined the formation of hydroxyapatite ($Ca_5(PO_4)_3OH$) on the sample surface after 3 days, suggesting it is a bioactive ceramic.

(Received October 26, 2022; Accepted January 14, 2023)

Keywords: Anorthite; CaF_2 addition amount, Sintering temperature, Mechanical and bioactive properties

1. Introduction

Anorthite (CaO, Al_2O_3, $2SiO_2$) is the lime-rich end member of the plagioclase feldspar series, it is a rare constituent in magmatic and metamorphic rocks. Due to its nontoxicity, chemical stability, low thermal expansion coefficient (4.82×10^{-6} K^{-1}), high thermal shock resistance, high creep resistance at high temperatures and low dielectric constant (6.2 at 1 MHz), anorthite is widely used in various technological applications such as electronics industry, industrial heat exchangers, photocatalysis and biomedical materials [1-5]. Thus, it is important to enhance the properties of anorthite, depending on the characteristics required for the intended application. Accordingly, many studies have been carried out to change their properties by modifying of synthesis method, coupling with other ceramics, our using additives (TiO_2, ZnO, B_2O_3, Na_2CO_3, …etc.) [6-9]. In the literature, calcium fluoride (CaF_2) as an additive has been proved to be a good candidate to improve the structural, mechanical, dielectric and bioactive properties of different ceramics ($ZnNb_2O_6$, $NdNbO_4$ ...etc.) and glass-ceramics ($CaO-Al_2O_3-MgO-SiO_2$, $SiO_2-Al_2O_3-CaO$, …etc.)[10-13]. Indeed, an optimum amount of CaF_2 can (1) increase the crystallization, (2) decrease the sintering temperature, (3) enhance the mechanical strength due to the augmentation of density (3) optimize hydroxyapatite formation on the surface of bioceramic [14-19]. Zhai et al. [20] investigated the influence of CaF_2 addition (2, 4, 6, and 8 wt.%) on the sintering temperature and microwave dielectric properties of $Li_2Mg_3TiO_6$ ceramic, prepared by the solid-state route.

* Corresponding author: belfennachedjamel@gmail.com
https://doi.org/10.15251/DJNB.2023.181.69

They report that the grain size has no apparent variation with CaF_2 content. However, 6 wt.% CaF_2 can reduce the sintering temperature from 1280 to 900 °C. Also, the 6 wt.% CaF_2-$Li_2Mg_3TiO_6$ ceramic treated at 1200 °C displays excellent microwave dielectric properties of dielectric constant (17.2), quality factor (76.800 GHz), and temperature coefficients of the resonant frequency (1.5 ppm/°C).

Until today, to the best of our knowledge, the different properties of anorthite ceramic as a function of CaF_2 additive have not been reported. Thus, in this study, the influence of CaF_2 content and sintering temperature on the densification, mechanical, structural, and bioactive properties of anorthite were investigated. The obtained ceramics were characterized by scanning electron microscopy (SEM), X-ray diffraction (XRD), Raman spectroscopy, Vickers microhardness, and in vitro bioactivity tests to determine their suitability for biomedical application.

2. Materials and Method

2.1. Samples preparation

Anorthite was fabricated by a modified milling system from kaolin (DD1) and calcium carbonate ($CaCO_3$) as Algerian raw materials, extracted from Guelma and Constantine, respectively. The device used in our milling system was manufactured at the laboratory using simple parts, as well as detailed elsewhere [21]. Many interesting published works have used this original milling system; they concern HA ceramics, wollastonite, diopside and others [21-25].

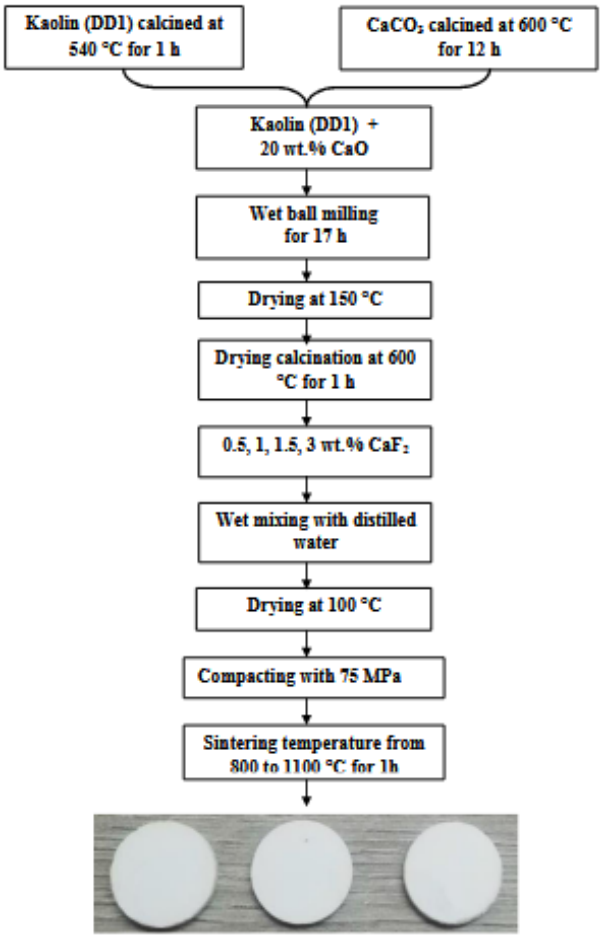

Fig. 1. *Schematic diagram describing the procedures of anorthite samples preparation.*

As shown in Fig. 1, the DD1 is properly crushed and calcined at 540 °C for 1 h to be later sieved at 200 μm. Then, 20 wt.% CaO of lime powderis added, which is obtained from $CaCO_3$ after its calcination at 600 °C for 12 h. This mixture was milled using a particular homemade vibratory milling system for 17 h and subsequently dried and calcined at 600 °C for 1 h. Further, 0.5, 1.5 and 3 wt.% CaF_2 have been added to the final powder, and denoted An0 (0 wt.%), An0.5 (0.5 wt.%), An1.5 (1.5 wt.%) and An_3 (3 wt.%). Then, the powder mixtures were compacted under 75 MPa using axial pressing. Finally, samples with dimensions of 13 × 2 mm^2 were dried at 100 °C for 24 h and sintered in the electrical furnace (Nabertherm LH 30/14, Lilienthal, Germany) at 800, 850, 900, 950, 1000 and 1100 °C for 1h.

2.2. Characterizations

The chemical composition of kaolin powder was determined by spectroscopic techniques, X-ray fluorescence (XRF) for metals and atomic absorption for alkaline earth metals.

The bulk density of samples was determined by the Archimedes method according to Eq.1.

$$\rho_{exp} = \frac{w_a}{w_a - w_b}\rho_b \quad (1)$$

where W_a is weight in the air, W_b is weight in the distilled water and ρb is the density of the distilled water. Also, a relative density was calculated based on Eq.2. The open pore was measured using the Archimedes buoyancy technique with dry weights.

$$(\%) = \frac{\rho_{exp}}{\rho_{theo}} \times 100 \quad (2)$$

where ρ_{theo} is the theoretical density of the sample.

The micro-hardness of the sintered samples was measured by the Vickers method with 15s dwell time using the Leitez Wetzlar machine (model 6844, Germany). The tensile tests of sintered samples were performed using a diametric compression test (FORM TEST SEIDNER D 79-40, Germany), and the proposed process is more detailed in [18]. The crystalline phase of the ceramics was identified by XRD (BRUKER, D8 ADVANCE, Germany). A Raman micro-spectrometer (BRUKER Raman SENTERRA R 200 L, Germany) was used in the interval of 200–1200 cm^{-1}. In the vibrational range of 500–4000 cm^{-1}, the functional groups present in the samples were defined by the Infrared spectrometer JASCO FT-IR 6300.

2.3. In vitro bioactivity tests

The in vitro properties of the sintered samples were assessed by their apatite (HA= $Ca_5(PO_4)3OH$) forming capacity in simulated body fluid (SBF, SBF-K9 type). The SBF was prepared according to Kokubo's protocol [26], by dissolving reagent-grade $CaCl_2$, NaCl, KCl, $MgCl_2.6H_2O$, $K_2HPO_4.3H_2O$, and $NaHCO_3$ into ultra-pure water, and buffered at pH=7.4 with tris-hydroxymethyl amino-methane and hydrochloric acid (HCl). Anorthite (An_0) and anorthite containing 1.5 wt.% CaF_2 ($An_{1.5}$) and sintered sample at 900 °C for 1 h, were soaked into 100 ml of SBF solution at 37 °C for 8 h, 3, 7, 14, and 21 days. After that, the samples were removed from the solution, gently washed with distilled water and dried for further analysis.

The flame photometers (JenwayPFP7, Germany) technique was used to evaluate the variations of calcium (Ca) and phosphorus (P) concentrations versus soaking time in all the reacted SBF solutions. The SBF solution was also monitored for changes in pH before and after in vitro test. Finally, the sample microstructure before and after soaking in SBF was characterized by XRD and SEM (Hitachi JSM-6301F, Japan).

3. Results and Discussion

3.1. Chemical composition and morphology of staring materials

The chemical composition of kaolin is given in Table I. It reveals that the major components were 43.60 wt.% SiO_2 and 36.30 wt.% Al_2O_3 and the main impurities are TiO_2, K_2O, CaO, Fe_2O_3,Na_2O, MgO and MnO.

Table 1. Chemical composition of kaolin DD1 (wt.%) by XRF analysis.

Oxides (%)	SiO_2	Al_2O_3	TiO_2	Fe_2O_3	K_2O	Na_2O	CaO	MgO	MnO	IL*
DD1	43.6	36.3	0.41	0.07	0.21	0.44	0.35	0.05	0.02	18.67

* Ignition loss (I.L.)

Figs. 2a and b display the SEM micrographs of kaolin (DD1) and calcite powder, respectively. The clay powder of DD1 shows nanorod shaped crystals with different lengths and diameter sizes, which are randomly oriented (Fig. 2a). Also, the morphology of the calcite powder presents a regular distribution of large agglomerates that are formed by small grains (Fig. 2b).

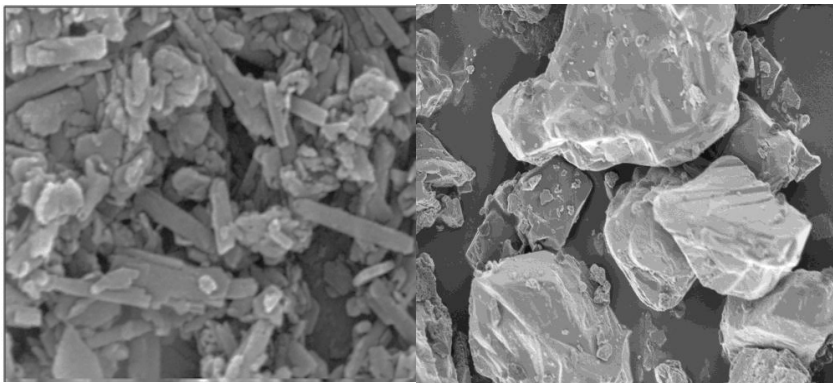

(a) (b)

Fig. 2. SEM micrographs of (a) kaolin (DD1) powder, (b) the ground limestone (CaCO3).

3.2. Densification Properties

Fig. 3 presents the variation of the bulk density of anorthite containing 0, 0.5, 1.5 and 3 wt.% CaF_2 versus sintering temperatures. All the samples behaved similarly, this is regardless of the CaF_2 content.

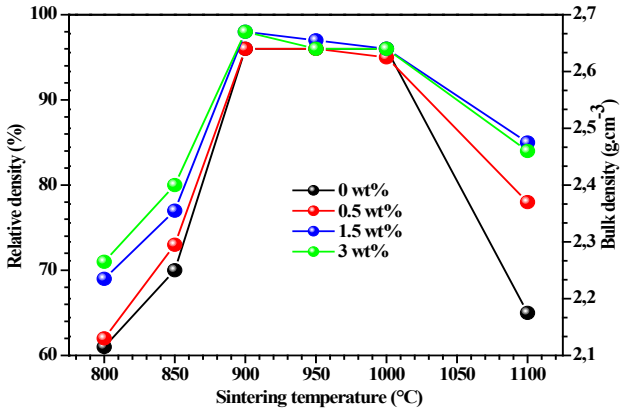

Fig. 3. *Effect of CaF_2 additions on relative density of anorthite samples sintered at different temperatures.*

It is seen that the density of the anortithe samples increased by sintering at 800-900 °C. The semi-stability was observed between 900 and 1000 °C, while a decrease in relative density occurred between 1000 and 1100 °C. Indeed, the curves shift consecutively towards higher relative density values from 0.5 to 3 wt.% CaF_2 additions. It reached its higher value (about 98% of the anorthite theoretical density) for samples containing 1.5 and 3 wt.% CaF_2. This increase in relative density at the first stage (800-900 °C) may also be due to grain growth. The presence of the liquid phase may also encourage small particles to move through it towards the concave regions of larger grains or particles in order to promote grain growth and therefore greater densification of the material. The higher sintering rate during the first stage for samples containing 0.5, 1.5 and 3 wt.% CaF_2 confirms the significant effect of this addition on the phase formation. It can be seen from Fig. 3 that, at the second stage (900-1000 °C), the relative density remained nearly constant for all samples. Indeed, the semi-stability was observed in this second stage which is probably due to the fact that sintering reached its final stage where the formed pores were closed and the increase in temperature cannot increase the sintering rate furthermore. Then, at the final stage (1000-1100 °C), a significant decrease in relative density was obtained for samples containing 0.5, 1.5 and 3 wt % CaF_2 and for samples without CaF_2 additions. This decrease in relative density may be due to the formation of volatile compounds in connection with some foreign impurities existing in the starting materials (kaolin). These compounds may lead to pore formation at higher temperatures. However, another interesting controlling parameter in favor of this significantly lower sintering temperature is the finer microstructure of the used kaolin powder. Indeed, the sintering temperature is generally closely related to the APS of starting powders and the preparation method.

Finally, samples sintered at 900 °C for 1 h are a good example that concerns the CaF_2 addition benefic effect on sintering. In reality, the bulk densities of samples containing 0.5, 1.5 and 3 wt.% CaF_2 were 2.64, 2.7 and 2.7 $g.cm^{-3}$, respectively. This relatively lower sintering temperature (900 °C) is significantly best when compared to other studies carried out on HA based bioceramics and particular materials [21-25].

3.3. Mechanical properties

The variation of apparent porosity of samples sintered at different temperatures is presented in Fig. 4, which shows that porosity decreases with the increase in sintering temperatures (800 and 1000 °C). For example, the porosity value varies from 42% to about 5% for samples without CaF_2 additions.

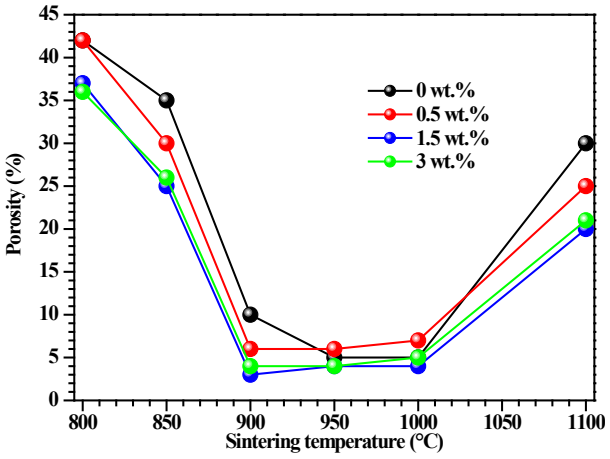

Fig. 4. *Porosity of anorthite samples containing different amounts of CaF_2 sintered at different temperatures.*

This decrease in porosity may be due to better sintering, native natural materials and closely related to the preparation method. However, in the samples containing different amounts of

CaF_2, the porosity decreases with the increase of CaF_2 in the range between 800 and 900 °C. For example, the samples containing 0.5, 1.5 and 3 wt.% CaF_2 sintered at 900 °C for 1 h had a porosity ratio of about 6%, 3% and 4%, respectively. These values may also be caused by the coalescence of formed smaller pores and the augmentation of grains size. This result confirms the significant effect of this CaF_2 addition on the sintering and the phase formation. Both flexural strength (3PFS) and Vickers micro-hardness (VMH) measurements are also of great importance stage for the preparation of the resistant anorthite. The VMH variation of samples containing 0, 0.5, 1.5 and 3 wt.% CaF_2 as a function of sintering temperature is given in Fig. 5.

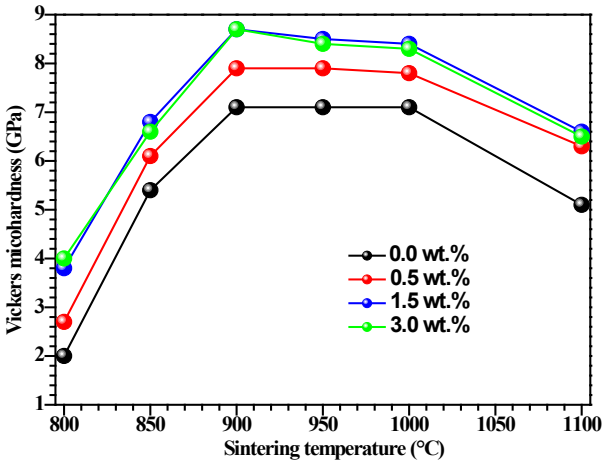

Fig. 5. *Vickers micro-hardness as a function of the sintering temperature for samples containing different CaF_2 percentages (wt.%).*

The curve behaviors in this figure may be divided into three main stages. Indeed, the first stage from 800 to 900 °C is characterized by the increase of VMH in all samples. In the second stage (900-1000 °C), a higher VMH value of ~8.7 GPa is reached for samples containing 1.5 wt.% CaF_2. But, the VMH of samples without addition and sintered at 900 °C is 7.1 GPa. Then, in the third stage when the sintering temperature becomes higher than 1000 °C, a remarkable decrease in VMH for samples is observed. It can also be noticed that the VMH curve behaves, more or less, similarly to that of the relative density. Indeed, the highest value was 8.7 GPa for samples containing 1.5 wt.% CaF_2 and sintered at 900 °C is significantly higher when compared to other studies. For example, VMH values of natural hydroxyapatite powders sintered at 1300 °C were (0.80 GPa) [27], (0.24 GPa) [28] and (4.70 GPa) [23]. Moreover, this value (8.7 GPa) is in good agreement with that of one of the hardest human being bones (4 GPa) [30]. The results obtained in the current study clearly confirm the importance of this value of VMH for the most resistant ceramics.

Furthermore, the variation of 3PFS values of the samples after sintering is illustrated in Fig. 6. All these drawn curves behave similarly. These behaviors may also be divided into three main stages. In the first stage (800 and 900 °C), all 3PFS values of samples increased sharply with sintering temperatures and gradually with CaF_2 contents.

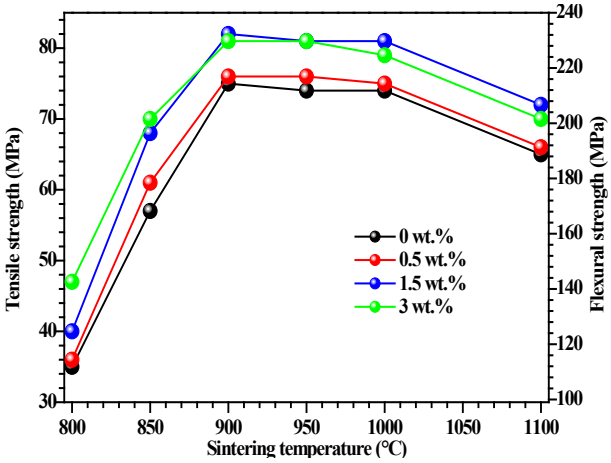

Fig. 6. *Tensile strength as function of CaF_2 percentages (wt.%) for samples sintered at different temperatures.*

However, the semi-stability was observed in the second stage with sintering temperatures between 900 and 1000 °C. Afterward, the 3PFS values of all samples sintered between 1000 and 1100 °C sharply decreased in the final stage with sintering temperatures. The 3PFS value reached its higher values (222 ± 32) MPa for samples containing 1.5 wt.% CaF_2 sintered at 900 °C for 1 h. However, the 3PFS values in samples containing 3 wt.% CaF_2 sintered at 900 °C were about 219 ± 32 MPa. Afterward, these values decrease in samples containing 0.5 and 0 wt.% CaF_2 to about 202 ± 32 MPa. The decrease in flexural strength at high temperatures may be due to the increase in pore sizes and porosity ratio coupled with the bloating effect. The shape, size and linkage trend of pores with each other played an important role in flexural strength. These equiaxed grains pores may decrease flexural strength. The above mentioned results confirm that the 3PFS values of sintered anorthite samples are closely related to the bulk densities. It can be said that these results underline the beneficial effect of CaF_2 additions on 3PFS and VMH values of anorthite samples.Finally, the maximum 3PBS (222 ± 32 MPa) is extremely higher than that reported in works carried out on HA-based ceramics. For example, *Nayak et al*. [30] have found that the addition of 2 w.% ZrO_2 into HA increased its 3PBS value from about 35 to 70 MPa. These obtained mechanical properties of anorthite samples are quite enough to qualify them as suitable to be used as bio-ceramics in many applications such as dental ceramics. Therefore, this elaborated anorthite may be well recommended as a good product for these purposes. Fortunately, this best achieved 3PBS value (about 222 MPa) for the $An_{1.5}$ sample is more than five times that of the HA value (about 44 MPa) [23].

3.4. Structural properties

Selected XRD patterns of samples containing different amounts of CaF_2 treated at 900 °C for 1 h are shown in Fig. 7

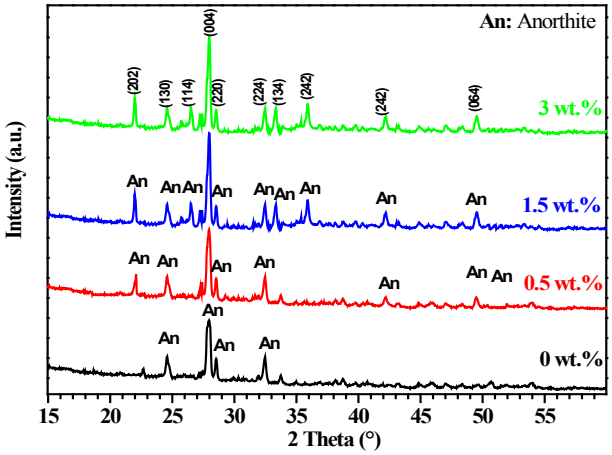

Fig. 7. *XRD spectra of anorthite samples containing different amounts of CaF_2 sintered at 900 °C for 1 h.*

All samples crystallize in the pure anorthite phase, which can be verified by the existence of $(\bar{2}02)$, (130), $(\bar{1}14)$, (220), $(\bar{2}24)$, $(\bar{1}34)$,$(\ \bar{2}\bar{4}2)$, $(2\bar{4}2)$, and $(0\bar{6}4)$ diffraction peaks (JCPDS 20-0020), and no other phases are identified. Further, as far as CaF_2 contents augment, the XRD results revealed the increase in the peaks intensity and the appearance of news peaks of anorthite, demonstrating the increase in the crystallinity. We conclude that the CaF_2 additions can activate the anorthite crystallization process at a relatively lower temperature.

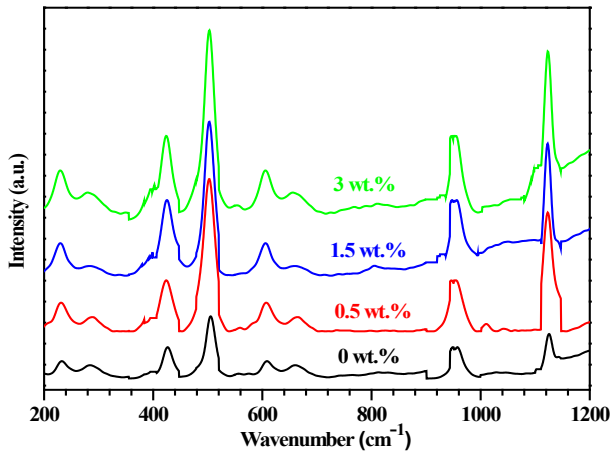

Fig. 8. *Raman spectra of anorthite samples sintered at 900 °C for 1 h.*

Fig. 8 shows the Raman spectrum of the samples containing different amounts of CaF_2, sintered at 900 °C. The spectra confirmed the presence of an anorthite phase with Raman bands located around 232, 287, 425, 505, 606, 664, 950 and 1126 cm^{-1}. The obvious Raman band locations are in agreement with anterior literature [24, 31-34]. In fact, from 200 to 400 cm^{-1}, the vibration may be assigned to lattice modes. The band at 425 cm^{-1} is associated with the T-O-T vibration. The 503 cm^{-1} band is ascribed to oxygen atoms movement along a line bisecting the T–O–T bond and creating a symmetric stretch. In the 600-800 cm^{-1} region, the bands are due to Al–Si vibrations within the tetrahedral units [31]. In the high-frequency region of the spectra, the modes are assigned to anti-symmetric stretching motions within the T-O-T bonds [v_s(T-O-T)]. Finally, the band at 1125 cm^{-1} comes from Si-O-Si anti-symmetric vibrations [34] On the other hand, from Fig. 8, we note that increasing CaF_2 content increases the Raman bands intensities which means the crystallinity improvement of anorthite. Also, there is no characteristic Raman

band of other phases. We can deduce that the Raman results are in good agreement with those obtained by XRD analysis. In addition, the FTIR spectra obtained for these ceramics are presented in Fig. 9.

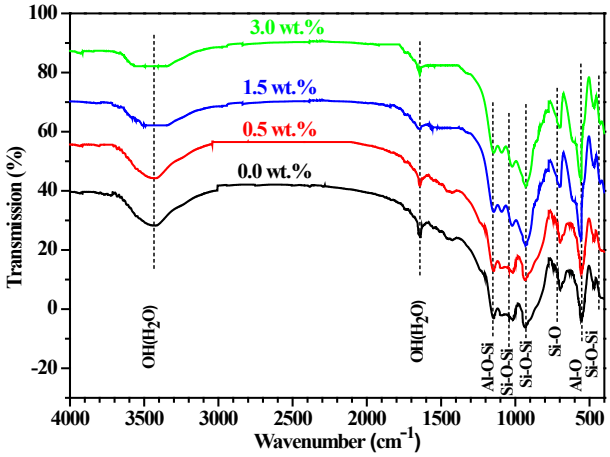

Fig. 9. *FT-IR spectra of anorthite samples sintered at 900 °C for 1 h.*

The last shows the characteristic bands of Si-O-Si (~ 466, 932 and 1011 cm^{-1}), Al-O (~ 556 cm^{-1}), Si-O (~697 cm^{-1}), Si-O-Al (~ 1150 cm^{-1}) and OH (~1640 and 3440 cm^{-1}). The obtained band positions are in agreement with the previous reports for the anorthite phase [26,27]. On the other hand, the intensity of the OH absorption band decreases when the CaF_2 increases.

3.5. In-vitro bioactivity assessment

In the following, we present the in vitro bioactivity results of An_0 and $An_{1.5}$ treated at 900 °C. This choice is based on the previous results. The good densification and mechanical proprieties of $An_{1.5}$ annealed at 900 °C compared to the other samples make it a promoter for the biomaterial application. The in vitro bioactivity of samples was studied by checking the pH, calcium (Ca) and phosphorous (P) concentrations variations in SBF solution as a function of soaking time. The study was also accomplished by analyzing the formed apatite layer (HA= $Ca_5(PO_4)_3OH$) at the samples surface by XRD and SEM techniques.

As can be observed in Fig. 10a, P ionic concentration in the solution decreased continuously for both samples. Almost all P ions migrated from SBF to the $An_{1.5}$ surface. Fig.10b shows the Ca concentration evolution followed a similar tendency for the two materials. The Ca has been released from An_0 surface for 8 h. After this time, the Ca concentrations decreased in SBF. While for the $An_{1.5}$, the maximum value for the Ca concentration in SBF was reached after 3 days, then decreased strongly and remained constant in the interval time 14-21 days.

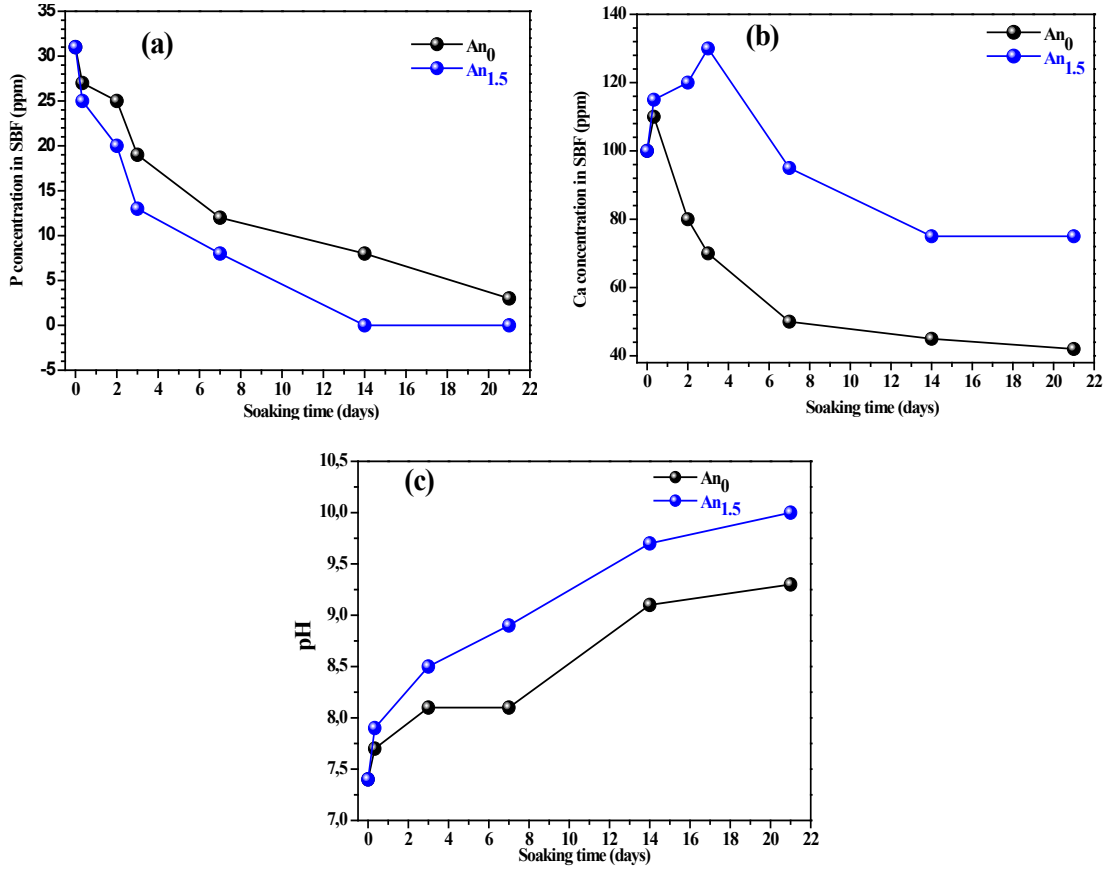

Fig. 10. *Evolutions of (a) P ion, (b) Ca ion concentrations and (c) pH in SBF solution versus soaking time for An_0 and $An_{1.5}$ ceramics.*

The variation of Ca and P concentrations in SBF shows that two processes occurred. The first process is the important release of Ca and P ions from the surface. The second process is the migration of Ca and P ions from SBF to the surface of anorthite linked to the precipitation of calcium phosphate (bone-like apatite) at the anorthite surface. Therefore, the decrease in the Ca and P concentrations in SBF is attributed to the rapid growth of the apatite at the anorthite surface that overcame the release rate of Ca and P ions to SBF [35,36]. These results indicate that the 1.5 w.% CaF_2 addition enhances the HA formation on the surface of anorthite. The pH measurement is important to study the dissolution process of the anorthite soaked in physiological solutions. As would be expected, pH variation with time was also similar for the both samples (Fig. 10c), increasing strongly after 8 h soaking time. The increase in pH of SBF is the result of ion exchanges between the protons H^+ in SBF and the anorthite modifying cations. For An_0, the pH value remains constant between 3 and 7 days. After that, the pH increased from a value of 8.1 to approximately 9.3 after 21 days. For $An_{1.5}$, it increases from 7.4 to 10 times after 21 days. In general, the pH variation with the soaking in time of the two samples shows that the increase in pH value of SBF was more noticeable for soaked $An_{1.5}$. The observed variations with time of the pH and the calcium concentration in SBF, for the An_0 and $An_{1.5}$ samples, are in agreement with the nucleation and growth mechanism of an apatite-like layer on Na_2O or $CaO–SiO_2$ bioactive glasses, proposed by Hench [37].

Figs.11a and b illustrate the XRD patterns of An_0 and $An_{1.5}$ before and after soaking in SBF solution for 8 h, 3, 7, 14 and 21 days. For An_0 before soaking in SBF (Fig.11a), the predominant phase identified is anorthite (JCPDS 20-0020). It is obvious that the characteristic peaks of anorthite decreased after 7 days of soaking. Furthermore, after 14 days of soaking in SBF, we note the appearance of two peaks at 26° and 32° corresponding to (002) and (211) planes of HA (JCPDS 09-0432), respectively. Fig. 11b illustrates the $An_{1.5}$ ceramic before soaking in SBF,

which shows the anorthite crystallizes phase. After 3 days of soaking, the spectrum exhibits the appearance of (002) plan of HA. This means that the formation of apatite on $An_{1.5}$ ceramic is faster than that on An_0. Also, it can be seen that increasing the days of soaking in SBF from 3 to 21 days leads to the appearance of two HA plans (211) and (212) and its intensification, indicating the augmentation of the crystallinity of HA on the surface of $An_{1.5}$ sample.

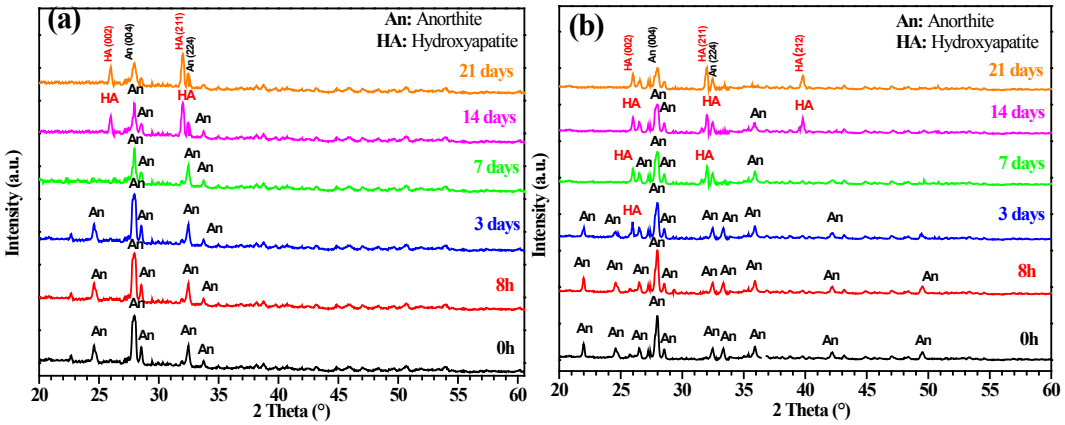

Fig. 11. *XRD patterns of (a) An_0 and (b) $An_{1.5}$ surfaces before and after soaking in SBF solution at different testing times.*

These XRD results prove the formation of HA on the surface of An_0 and $An_{1.5}$ samples and that 1 wt.% CaF_2 addition accelerates and improves its formation and crystallization on the surface. As the samples dipped in SBF solution, some chemical reaction takes place between the constituents of ceramics and ions present in SBF solution with time which leads to the formation of an HA crystalline layer on its surface. Therefore, their formation strongly depends on the chemical composition of the samples.

Typical SEM images of An_0 and $An_{1.5}$ samples sintered at 900 °C for 1 h, before and after soaking in SBF solution for 14 days are given in Fig. 12. Before soaking, $An_{1.5}$ illustrates the formation of larger amounts of anorthite compared to An_0 which must be favored by the presence of CaF_2 particles (Figs. 12a and c). This is agreed with those presented in the XRD and Raman analysis. At the same time, the absence of macro-defects such as cracks has been remarked, these features are important for the fabrication quality of this resistant anorthite based ceramics. Besides, the soaking in SBF solution for 14 days greatly affects the morphological shape of An_0 and $An_{1.5}$ (Fig. 12b and d). This latter reveals homogeneous surface morphology. An_0 surface was completely covered by particular nano-sized crystallites (rice shaped) of HA layer (Fig. 12b). However, the $An_{1.5}$ surface shows the continuous layer of dense and nanorods shaped grains attributed to the HA (Fig. 12d). Thus, the SEM analysis confirms the production of HA on the surface of An_0 and $An_{1.5}$ soaking in SBF solution for 14 days and that CaF_2 addition favorite this process. This is in agreement with the XRD results.

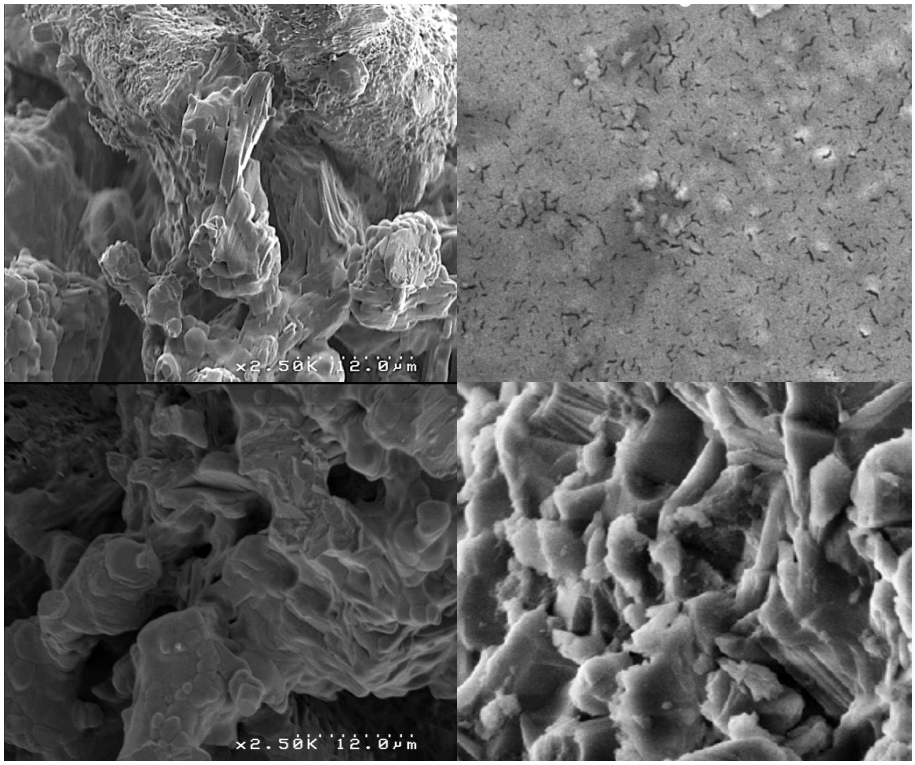

Fig. 12. *SEM micrographs of (a-b) An_0 and (c-d) $An_{1.5}$ surfaces before and after 14 days soaking in SBF.*

4. Conclusion

Anorthite ($2SiO_2 \cdot Al_2O_3 \cdot CaO$) and anorthite with CaF_2 (0.5–3 wt.%) additions ceramics were obtained by solid-state reaction from Algerian raw materials. The samples were sintered at different temperatures (800–1100 °C) for 1 h in air. The effect of these two parameters on the densification, mechanical, and bioactive properties of resistant anortithe was studied, and the following conclusions were drawn:

The relative density, porosity, VMH and 3PFS values of the samples were varied in three stages as a function of sintering temperatures. The relative density is in the range of 61-98%, it reached the maximum value about 98 % for anorthite containing 1.5 and 3 wt.% CaF_2 at 900 °C. By contrast, at this temperature, the porosity illustrated a minimum value of 3% for anorthite with 1.5 wt.% CaF_2. A higher VMH value of about 8.7 GPa was obtained for this latter but treated at 900, 950 and 1000 °C. Also, the 3PFS achieved its higher values of 222 MPa for samples containing 1.5 wt.% CaF_2 and sintered at 900 °C. These different results mean that 1.5 wt.% CaF_2 and 900 °C are the optimum parameters. The XRD and Raman results of the samples annealed at 900 °C showed the presence of an anorthite phase, and that the CaF_2 content improves its crystallinity. Finally, the in vitro bioactivity assessment of anorthite with 1.5 wt.% CaF_2 showed the formation of HA on the surface, after immersion in SBF between 3 and 21 days, thus indicating this developed ceramic is bioactive, thus suitable for biomaterials applications.

References

[1] J. Liu, Y. Zhang, Z. Su, D. Huang, D. Xu, M. Lu, S. Liu,T. Jiang, Energy Fuels 35, 12425−12435 (2021); https://doi.org/10.1021/acs.energyfuels.1c01196

[2] S. Csaki, F. Lukac, T. Hulan, J. Veverka, M. Knapek, J. Eur. Ceram. Soc. 41, 4618−4624

(2021); https://doi.org/10.1016/j.jeurceramsoc.2021.03.004

[3] J. Liu, Y. Zhang,Z. Su, D. Huang, D.Xu, M. Lu, S. Liu, T. Jiang, J. Am. Chem. Soc. 35, 12435 (2021); https://doi.org/10.1021/acs.energyfuels.1c01196

[4] K. Tabit, H. Hajjou, M. Waqif, L. Saâdi, Ceram. Int. 46, 7558 (2020); https://doi.org/10.1016/j.ceramint.2019.11.254

[5] V.V. Shekhovtsov, N.K. Skripnikova, M.A. Semenovykh, O.G. Volokitin, Glass. Cerm.78, 241 (2021); https://doi.org/10.1007/s10717-021-00386-w

[6] D. P. Mukherjee, S. K. Das, Ceram. Int. 40(3), 4127-4134(2014); https://doi.org/10.1016/j.ceramint.2013.08.067

[7] E. Montoya-Quesada, M. A.Villaquirán-Caicedo, R.M. Gutiérrez, J.Muñoz-Saldaña, Ceram. Int. 46(4), 4322-4328 (2020); https://doi.org/10.1016/j.ceramint.2019.10.154

[8] A.Schusser, M.J.Pascual, A.Prange, A.Durán, R.Conradt, Ceram. Int. 39(4), 3753-3758(2013); https://doi.org/10.1016/j.ceramint.2012.10.213

[9] Yi-Chong Liao, Chi-Yen Huang, Ceram. Int. 38(5), 4415-4420 (2012); https://doi.org/10.1016/j.ceramint.2012.01.080

[10] Y.C. Zhang, Z.X. Yue, Z.L. Gui, L.T. Li, Ceram. Int. 29(5), 555-559 (2003); https://doi.org/10.1016/S0272-8842(02)00202-X

[11] P. Zhang, T. Wang, W. Xia, L. Li, J. Alloys Compd. 535,1-4 (2012); https://doi.org/10.1016/j.jallcom.2012.04.090

[12] F. Pei, G. Zhu, P. Li, H. Guo, P. Yang, Ceram. Int. 46 (11) , 17825-17835 (2020); https://doi.org/10.1016/j.ceramint.2020.04.089

[13] D. P.Mukherjee, S. K. Das, Ceram. Int. 39(1), 571-578(2013); https://doi.org/10.1016/j.ceramint.2012.06.066

[14] M. Esmaili, M.R. Nilforoushan, M. Tayebi, E. Aghaie, Ceram. Int. 47, 17435−17444 (2021); https://doi.org/10.1016/j.ceramint.2021.03.060

[15] W.N.W. Jusoh, K.A. Matori, M. H. M. Zaid, N .Zainuddin, M. Z. A. Khiri, N. A. A. Rahman, R. A. Jalil, E .Kul, Ceramics Silikáty 64, 447−459 (2020).

[16] S. Prasad, S. Ganisetti, A. Jana, S. Kant, P.K. Sinha, S. Tripathy, K. Illath, T.G. Ajithkumar, K. Annapurna, A.R. Allu, K. Biswas, J. Alloys. Compd. 831, 154704 (2020); https://doi.org/10.1016/j.jallcom.2020.154704

[17] L. Deng, X. Zhang, M. Zhang, X. Jia, J. Non. Cryst. Solids. 500, 310−316 (2018); https://doi.org/10.1016/j.jnoncrysol.2018.08.018

[18] H.W. Kima, Y.J. Noha, Y.H. Koha, H.E. Kima, H.M. Kim, Biomaterials 23, 4113−4121 (2002); https://doi.org/10.1016/S0142-9612(02)00150-3

[19] Y.C. Zhang, Z.X. Yue, Z.L. Gui, L.T. Li, Ceram. Int. 29, 555-559 (2003); https://doi.org/10.1016/S0272-8842(02)00202-X

[20] S. Zhai, P. Liu, Z. Fu, J. Li, J. Mater. Sci: Mater. Electron. 30, 5404-5409 (2019); https://doi.org/10.1007/s10854-019-00833-z

[21] E. Harabi, A. Harabi, F.Z. Mezahi, S. Zouai, N. Karboua, S. Chehalatt, Des. Wat. Treat. 57, 5302 (2016); https://doi.org/10.1080/19443994.2015.1022000

[22] A. Harabi, E. Harabi, S. Chehalatt, S. Zouai, N. Karboua, L. Foughali, Des. Wat. Treat. 57, 5309 (2016); https://doi.org/10.1080/19443994.2015.1021997

[23] E. Harabi, A. Harabi, L. Foughali, S. Chehlatt, S. Zouai, F.Z. Mezahi, Acta. Phys. Pol 127, 1163 (2015); https://doi.org/10.12693/APhysPolA.127.1161

[24] S. Zaiou, A. Harabi, E. Harabi, A. Guechi, N. Karboua, M.T. Benhassine, S. Zouai, F. Guerfa, Cerâmica. 62, 322 (2016); https://doi.org/10.1590/0366-69132016623642015

[25] A. Harabi, S. Zaiou, A. Guechi, L. Foughali, E. Harabi, N.E. Karboua, S. Zouai, F.Z. Mezahi, F. Guerfa, Cerâmica. 63, 317 (2017); https://doi.org/10.1590/0366-69132017633672020

[26] T. Kokubo, H. Kushitani, S. Sakka, T. Kitsugi, T. Yamamuro, J. Biomed. Mater. Res. 24, 734 (1990); https://doi.org/10.1002/jbm.820240607

[27] F.Z. Mezahi, A. Harabi, S. Zouai, S. Achour, D. Bernache-Assollant, J. Mater. Sci. 493, 248

(2005).

[28] S. Salman, O. Gunduz, S. Yilmaz, M.L. Ovecoglu, R.L. Snyde, S. Agathopoulos, F.N. Oktar, Ceram. Int. 35, 2971 (2009); https://doi.org/10.1016/j.ceramint.2009.04.004

[29] H. Ming, Z.S. Ren, Z.X. Hua, J. Mater. Sci. 22, 393 (2011); https://doi.org/10.1007/s10854-010-0148-1

[30] Y. Nayak, R.P. Rana, S.K. Pratihar, S. Bhattacharyya, J. Mater. Sci. A 210, 2444 (2008).

[31] A.A. Zolotarev, S.V. Krivovichev, T.L. Panikorovskii, V.V. Gurzhiy, V.N. Bocharov, M.A. Rassomakhin, Minerals. 9, 570 (2019); https://doi.org/10.3390/min9100570

[32] T. Xie, G.R. Osinski, S.R. Shieh, Meteoritics. Planetary. Science. 56, 1651 (2021); https://doi.org/10.1142/11930

[33] S. Sharma, B. Simons, H.S. Yoder, Am. Mineral. 68, 1125 (1983).

[34] R. Le Parc, B. Champagnon, J. Dianoux, P. Jarry, V. Martinez, J. Non. Cryst. Solids. 323, 161 (2003); https://doi.org/10.1016/S0022-3093(03)00302-8

[35] P. Sepulveda, J.R. Jones, L.L. Hench, J. Biomed. Mater. Res. 61, 311 (2002); https://doi.org/10.1002/jbm.10207

[36] J. Roman, S. Padilla, M. Vallet-Regi, Chem. Mater. 15, 806 (2003); https://doi.org/10.1021/cm021325c

[37] L.L. Hench, J. Am. Ceram. Soc. 74, 1510 (1991); https://doi.org/10.1111/j.1151-2916.1991.tb07132.x